

- Coffin MF and Eldholm O (1994) Large igneous provinces: crustal structure, dimensions, and external consequences. *Reviews of Geophysics* 32: 1–36.
- Cox KG (1980) A model for flood basalt vulcanism. *Journal of Petrology* 21: 629–650.
- Davies GF (2000) *Dynamic Earth: Plates, Plumes and Mantle Convection*. New York: Cambridge University Press.
- Duncan RA and Richards MA (1991) Hotspots, mantle plumes, flood basalts, and true polar wander. *Reviews of Geophysics* 29: 31–50.
- Hinz K (1981) A hypothesis on terrestrial catastrophes: wedges of very thick oceanward dipping layers beneath passive continental margins – their origin and paleoenvironmental significance. *Geologisches Jahrbuch* E22: 3–28.
- Macdougall JD (ed.) (1989) *Continental Flood Basalts*. Dordrecht: Kluwer Academic Publishers.
- Mahoney JJ and Coffin MF (eds) (1997) *Large Igneous Provinces: Continental, Oceanic, and Planetary Flood Volcanism*. Washington: American Geophysical Union Geophysical Monograph 100.
- Morgan (1981) Hotspot tracks and the opening of the Atlantic and Indian oceans. In: Emiliani C (ed.) *The Oceanic Lithosphere, The Sea*, Vol. 7, pp. 443–487. New York: John Wiley.
- Richards MA, Duncan RA and Courtillot VE (1989) Flood basalts and hot-spot tracks: plume heads and tails. *Science* 246: 103–107.
- Saunders AD, Tarney J, Kerr AC and Kent RW (1996) The formation and fate of large oceanic igneous provinces. *Lithos* 37: 81–95.
- Sigurdsson H, Houghton BF, McNutt SR, Rymer H and Stix J (eds) (2000) *Encyclopedia of Volcanoes* San Diego: Academic Press: 1147pp.
- Sleep NH (1992) Hotspot volcanism and mantle plumes. *Annual Review of Earth and Planetary Science* 20: 19–43.
- White R and McKenzie D (1989) Magmatism at rift zones: the generation of volcanic continental margins and flood basalts. *Journal of Geophysical Research* 94: 7685–7729.
- White RS and McKenzie D (1995) Mantle plumes and flood basalts. *Journal of Geophysical Research* 100: 17543–17585.

INDIAN OCEAN EQUATORIAL CURRENTS

M. Fieux, Université Pierre et Marie Curie,
Paris Cedex, France

Copyright © 2001 Academic Press

doi:10.1006/rwos.2001.0367

Introduction

Dynamically the equatorial area is a singular region on the earth because the Coriolis force is small, vanishing exactly at the equator. This results in a current structure that differs from that at other latitudes. Moreover, the equatorial current system of the Indian Ocean is entirely different from the current system found near the equator in the Pacific and Atlantic. This is principally due to its different wind forcing, which is described in the first section below. The systems of strictly equatorial currents at surface and at depth are reviewed in the second section. The third and fourth sections describe the North-East and South-West Monsoon Currents, north of the Equator, and the South Equatorial Countercurrent and the South Equatorial Current, south of the Equator.

The Atmospheric Circulation over the Equatorial Indian Ocean

The winds over the tropical Indian Ocean are quite different from the winds over the Atlantic and the

Pacific tropical oceans, where the NE and SE trade winds blow always in the same direction. Instead, the Indian Ocean (**Figure 1**), north of 10°S, is under the influence of a monsoonal circulation, with complete reversal of the winds twice a year. The winter monsoon (December–March) blows from the NE in the Northern Hemisphere and from the NW south of the Equator toward the intertropical convergence zone (ITCZ) located near 10°S. The change in direction at the Equator comes from the change of sign of the Coriolis force. The summer monsoon (June–September) blows from the SW in the Northern Hemisphere in continuity with the SE trade winds of the Southern Hemisphere, particularly in the western part of the equatorial ocean. The winds are stronger during the summer monsoon season. At the equator, during the monsoons, the winds have a preponderant meridional component, southward during the winter monsoon and northward during the summer monsoon, particularly near the western boundary. The result is a strong annual cycle in the meridional component of the winds corresponding to the reversals between the NE and the SW monsoons, particularly in the western region along the Somali coast where the winds are the strongest.

Between the monsoons, during the two transition periods, at the Equator, moderate eastward winds blow in spring (April–May) and in fall (October–November), with maxima between 70°E and 90°E

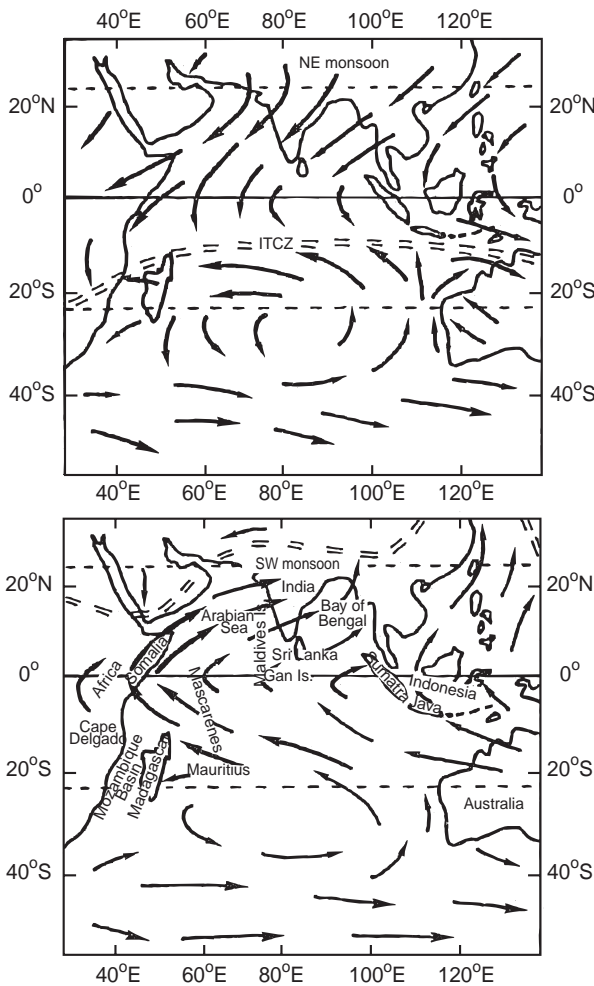


Figure 1 Winds over the Indian Ocean during the NE monsoon (A) and during the SW monsoon (B) with locations used in the text.

(Figure 2). They could blow into one or several eastward bursts with a large seasonal and inter-annual variability. During the NE monsoon, the mean zonal component of the wind is weakly westward west of 80°E, increasing in strength near the Somali coast. During the SW monsoon, the zonal components of the winds is weakly westward between 60°E and 70°E; west and east of that region, they are weakly eastward with a maximum between 80°E and 90°E. As a result, the annual mean zonal wind is eastward, the opposite of what is found in the other equatorial oceans, and is maximum around 80°E to 85°E.

This particular wind regime is dominated by an annual and a semiannual cycle with similar amplitudes for the zonal components. The amplitude of the annual component is maximum near the western boundary associated with the stronger monsoon winds off Somalia. Relative annual component

maxima are also found near 82°E and near the eastern boundary due to the southward monsoon winds extension south of Sri Lanka and along the Indonesian coast.

In contrast, the semiannual component of the equatorial zonal winds has a simple structure with a single maximum in the central ocean between 60°E and 80°E during spring and fall.

Currents at the Equator

Currents in the Extreme West, along the Somali Coast

Compared to the other major oceans, there are very few direct current measurements in the Indian Ocean and most of the surface currents information comes from the ship drifts and recently from satellite-tracked drifting buoys.

Along the Somali Coast, as seen above, the annual period is the dominant variability in the wind forcing. It is only relatively recently (1984–1986) that long-term direct current measurements were carried out at the equator within 200 km off the Somali coast. Above 150 m they show a seasonally reversing flow in phase with the NE and the SW monsoons, but a striking asymmetry between both monsoon seasons. While during the stronger SW summer monsoon the north-eastward Somali Current decays monotonically in the vertical, during the weaker NE winter monsoon the south-westward surface current is limited to the surface layer and a north-eastward countercurrent exists between about 150 m and 400 m, remnant of the SW monsoon current, followed again by weak south-westward current underneath down to about 1000 m (Figure 3). This sliced structure is confined to the equatorial region corresponding to the equatorial waveguide.

Surface Currents at the Equator, East of 52°E

Ship-drift climatology indicates that, at the equator, the surface currents reverse direction four times a year. During the two transition periods, under the influence of the equatorial eastward winds, a strong surface eastward jet (known as the ‘Wyrтки jet’ because Klaus Wyrтки first identified it by looking at different shipdrift atlases in the 1960s) sets up in a narrow band, trapped in the equatorial wave guide within 2–3° of the equator (Figure 4). The Wyrтки jet exists mostly in the central and eastern regions and disappears in the western part where the currents have a strong meridional component as shown above. Owing to the efficiency with which zonal winds can accelerate zonal currents at the

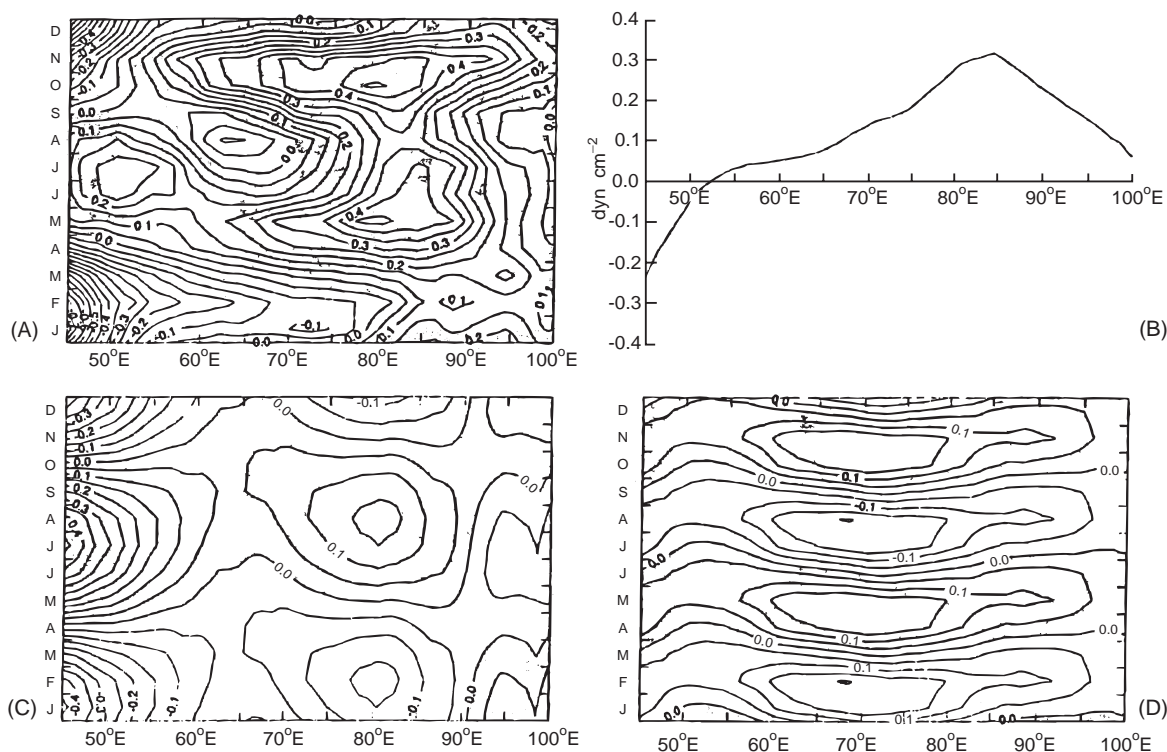


Figure 2 Longitude time plots of equatorial zonal wind stress averaged from 1°S to 1°N, determined from the FSU pseudostress climatology for the period 1970–1996: (A) the total wind in dyn cm^{-2} ; (B) time-averaged mean zonal wind stress; (C) annual zonal wind stress component; (D) semiannual zonal wind stress component. Contour interval is 0.05 dyn cm^{-2} , eastward wind stress regions are shaded. (From W Han, JP McCreary, DLT Anderson, AJ Mariano (1999) Dynamics of the eastern surface jets in the equatorial Indian Ocean, *Journal of Physical Oceanography* 29: 2191–2209, (1999) copyright by the American Meteorological Society.)

equator where the Coriolis force disappears, the current speed can reach 1 m s^{-1} . The ship drift climatology indicates roughly the same strength for the two jets, with the October–November one (1 m s^{-1}) slightly stronger than the April–May one (0.90 m s^{-1}). As there is a large seasonal and interannual variability in the eastward winds, strong currents could be found in April–May instead of October–November during some years.

At the equator, in the middle of the Indian Ocean, the first long-term current measurements (1973–1975), near Gan Island ($73^{\circ}10\text{E}-0^{\circ}41\text{S}$), show energetic eastward currents throughout the upper 100 m mixed layer in phase with the zonal eastward component of local winds during the two transition periods between the monsoons (Figures 5, 6). The establishment of this eastward jet could be explained through eastward-propagating Kelvin waves triggered by the eastward-going winds during the transition periods. The stopping of the jet is thought to be the result of the reflection of the eastward-propagating Kelvin waves on the eastern coast into westward-propagating equatorially trapped Rossby waves that progressively impede

the jet from east to west. This has been observed with drifting buoys (Figure 7). The eastward currents at the equator are convergent (contrary to the westward currents). Consequently, drifting buoys launched in the jet stay in it and are a good means of observing its variability. In Figure 8 the drifting buoys were entrained into the May jet. They then stopped during the SW monsoon drifting slowly south of the equator and were taken up again eastwards into the November jet.

Between the strong eastward flow periods, the equatorial surface currents are westward and much weaker (Figures 4 and 6). The associated change of current direction during each transition period produces semiannual variations in the thermocline depth and sea level. During periods of eastward flow when warm water is carried toward the east, the thermocline deepens off Sumatra and rises off Africa, corresponding to opposite displacements of the sea surface. Strong eastward flow at the equator entrains a surface convergence and as a result a downwelling in the upper layer, contrary to what is found in the other oceans. It is only during

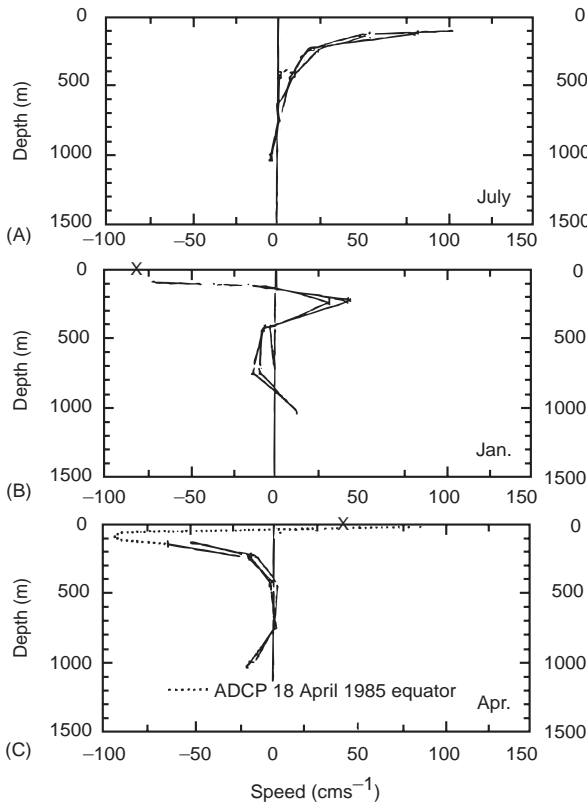


Figure 3 Monthly mean current profiles observed on three moorings in the Somali current at the equator during the NE monsoon (January 1985), the SW monsoon (July 1985), and during the transition period (April 1985); monthly mean of component parallel to coast. The crosses at the surface are historical ship drift data from Cutler and Swallow (1984). The dotted near-surface profile in April is from the ship mounted acoustic Doppler current profiler. (From F Schott (1986). Seasonal variation of cross-equatorial flow in the Somali current *Journal of Geophysical Research* 91(C9): 10581–10584, copyright by the American Geophysical Union.)

the weak westward flow that there is a weak upwelling.

Long-term direct current measurements carried between Sri Lanka and 0°45'S, in 1993–1994, reveal a large seasonal asymmetry that year in the semi-

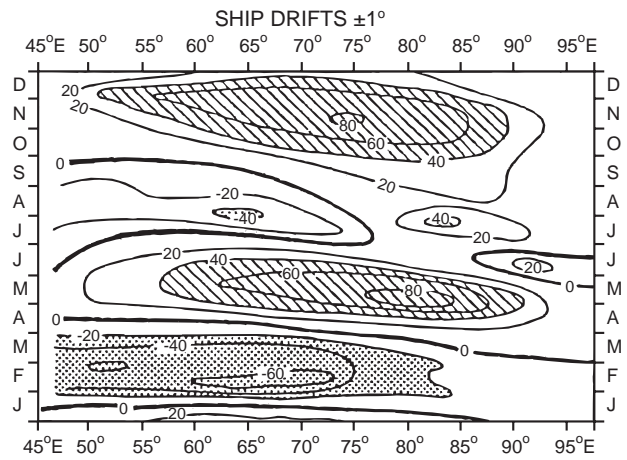


Figure 4 Mean ship drift estimates of the current between 1°N and 1°S in cm s^{-1} . Dots correspond to westward currents and stripes to eastward currents. (From G Reverdin (1987). The upper equatorial Indian Ocean: The climatological seasonal cycle. *Journal of Physical Oceanography* 17: 903–927, copyright by the American Meteorological Society.)

annual eastward jet transport, with 35 Sv in November 1993 (surface velocities exceed 1.3 m s^{-1}) and only 5 Sv in May 1994. These transports were calculated with a lower boundary sets at 200 m as, sometimes, the eastward currents are not confined to one core but extend into the ray-like structures of the equatorial waves that continue to greater depths as in November 1993 (Figure 9). This large variability is due to a large seasonal and interannual variability of the zonal winds partly related to the Southern Oscillation. For example, during the El Niño of the century in 1997, the equatorial eastward winds in the Indian Ocean completely disappeared in October–November and were replaced by westward winds.

Numerical model results show that direct wind forcing is the dominant forcing mechanism of the equatorial surface jets. The semiannual response of the current to the wind is nearly three times as

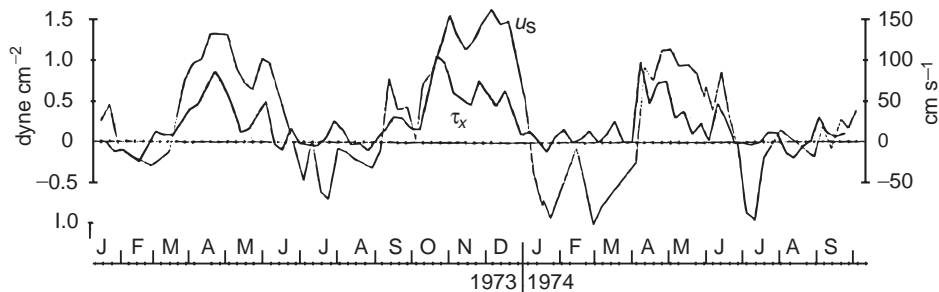


Figure 5 Comparison of weekly average zonal wind stress (τ_x) in dyne s^{-2} and surface zonal currents (u_s) in cm s^{-1} at Gan Island ($73^\circ 10'E-0^\circ 41'S$) in 1973–1975 (Reprinted from RA Knox. On a long series of measurements of Indian Ocean equatorial currents near Addu Atoll, copyright 1976, *Deep-Sea Research* 23: 211–221, with permission from Elsevier Science.)

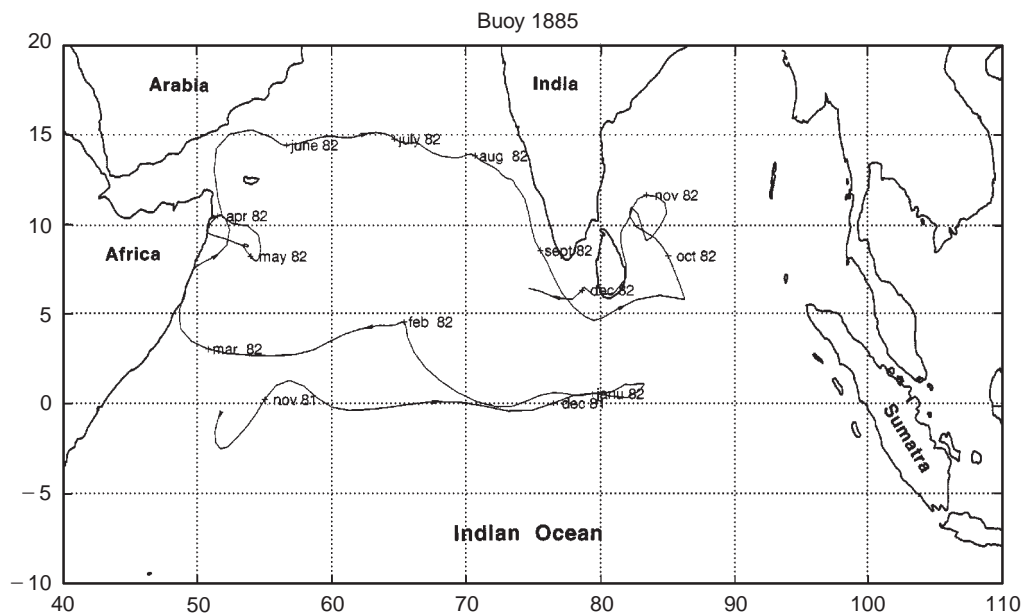


Figure 6 Trajectory of one drifting buoy (drogued at 20m) entrained eastward into the equatorial Wyrтки jet in November–December 1981, then in the reversal in December–January, crossing the Arabian Sea, and undergoing the seasonal reversal of the current south of Sri Lanka. (From M. Fieux (1987) *Océan Indien et Mousson 'Unesco Anton Bruun Lecture'* 15 pages, unpublished manuscript.)

strong as the annual one, despite similar amplitudes in the corresponding wind components. This is due to the simpler zonal structure of the semiannual wind and to the resonance of the basin to the semiannual component. The mixed layer shear flow seems also to enhance the semiannual response. The jet is strengthened when the mixed layer is reduced, particularly when the precipitation during the northern hemisphere summer and fall thins the mixed layer in the eastern ocean and so could strengthen the November jet in the east. The reflection of equatorial Kelvin waves into westward going Rossby waves at the eastern boundary is also important in weakening and even canceling the directly forced eastward jet about 2 months after the wind onset. The presence of the Maldives islands blocks part of the equatorially trapped waves. The effect on the semiannual waves is to weaken both jets, and the effect on the annual waves tends to weaken the May jet and to strengthen the November jet.

Currents at Depth at the Equator

It is only during the NE monsoon, the season when the large-scale wind structure resembles the Pacific and the Atlantic ones, that a similar eastward equatorial undercurrent (EUC) embedded in the thermocline exists. Observations of the equatorial undercurrent are scarce. It was first observed during the International Indian Ocean Expedition (IIOE) in March–April 1963, between 53°E and 92°E, with

speeds up to 0.8 m s^{-1} , then at Gan Island (73°E) in March 1973 with velocities of up to 1 m s^{-1} , but not the following year. In 1975 and 1976, it was found from January extending into May–June at 55°30'E with observed speeds reaching 0.8 m s^{-1} in February and March at the end of the NE monsoon (Figure 10). Direct measurements give a maximum transport of 17 Sv, in March–April 1994, at the longitude of Sri Lanka (80°30'E) (Figure 9). It is confined between 2°30'N–2°30'S with slight meandering and is weak east of 80°E. Its core is around 100 m in the upper equatorial thermocline. During the NE monsoon, it flows under a weak westward current until April–May when the eastward Wyrтки jet starts, then the whole upper layer flows eastward. It stops in May–June but surprisingly, in 1994, it reappeared in August.

The existence of the EUC is related to equatorial westward winds, which force a westward surface current that builds up a zonal pressure gradient below the mixed layer that maintains the eastward undercurrent. The slope of the sea surface is opposite to the slope of the thermocline. The reappearance of the undercurrent in August 1994 is effectively related to anomalous onset of westward winds in the eastern part of the ocean, during May and June 1994. They force a westward surface current, again building a subsurface zonal pressure gradient, and thus an eastward undercurrent reappeared with some delay in August 1994.

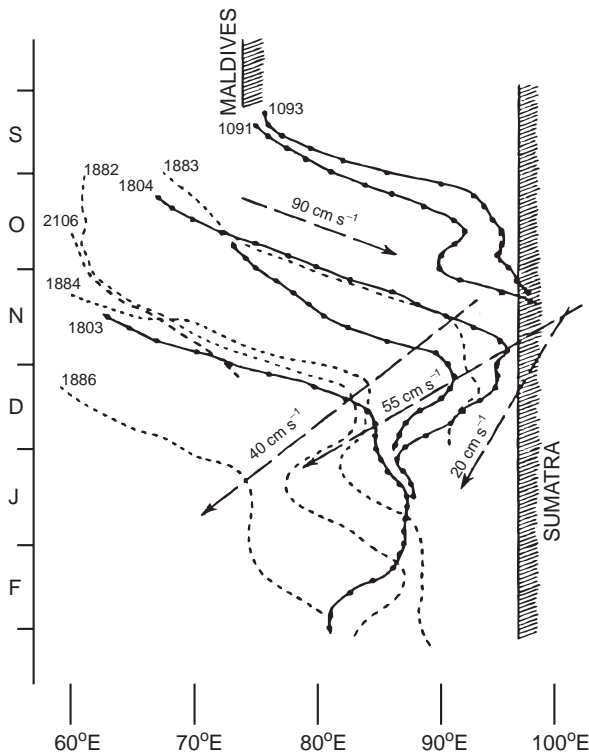


Figure 7 Drifting buoy trajectories between 60°E and Sumatra during the period of September–February. Full lines are for 1979–1980 and dashed lines are for 1980–1981. Dashed arrows indicate different speeds on this time–longitude diagram. During the first year the reversal propagation speed toward the west was around 55 cm s^{-1} , and around 40 cm s^{-1} during the second year. (From G Reverdin, M Fieux, J Gonella and J Luyten (1983) Free drifting buoy measurements in the Indian Ocean equatorial jet. In: Nihoul JCJ (ed.) *Hydrodynamics of the Equatorial Ocean*. Amsterdam: Elsevier Science, 99–120.)

In 1976, current profiles show that the vertical velocity structure in the vicinity of the equator is characterized by small vertical scales of order of 50–100 m in the upper layer increasing with depth throughout the water column. This deep jetlike structure is trapped to within 1° of the Equator and has a timescale of the order of several months.

One-year current-meter measurements made at 200 m, 500 m, and 750 m at the Equator, between 48°E and 62°E , and recently at 80°E , present a dominant semiannual reversal of the zonal component at all depths, much deeper than could be explained by direct wind forcing (Figure 11). Furthermore, these reversals do not happen at the same time at different depths. This seasonal cycle, with larger vertical scales, has been shown to penetrate vertically. The measurements suggest a mixture of equatorial Kelvin waves and long equatorial Rossby waves propagating downward from the surface where they are forced by the winds. The

zonal velocity shows upward phase propagation, and downward energy propagation away from the surface. The behavior of the zonal currents is characteristic of an eastward-propagating equatorial Kelvin wave and a westward-propagating long equatorial Rossby wave. The ratio of the semi-annual energy in the east current component to that in the north component is 40 to 1. This shows how much the equatorial ocean is a barrier to the meridional motions.

Currents North of the Equator

South of Sri Lanka

North of the Equator, the monsoon forcing drives a general eastward flow, the South-west Monsoon Current (SMC), during the fully developed SW monsoon, and a general westward flow, the North-east Monsoon Current (NMC), during the NE monsoon, extending south to about 2°S in January–February. The exchanges between the Arabian Sea and the Bay of Bengal are restricted to the south of India and Sri Lanka. Drifting-buoy trajectories show the seasonal current reversal in that restricted region (Figure 6).

Direct observations carried out in 1991–1994 south of Sri Lanka show that the monsoon currents are mostly confined in the upper 100 m. In August 1993, the eastward SMC extended to the equator and retracted north of $4^\circ 30'\text{N}$ in September. It was replaced in October by the westward NMC, extending south to about 2°N , with speeds between 0.3 and 0.8 m s^{-1} (Figure 9). Shipdrifts show that, around the Maldives, the NMC splits into a branch that bends south-westward and a branch that follows the western coast of India, bringing low-salinity Bay of Bengal water into the Arabian Sea. The NMC maximum flow lies north of 4°N with a mean transport of 10–12 Sv (Figure 12). In May the current reverses eastwards into the SMC again. The SMC transport reaches about 8–10 Sv with speeds up to 0.75 m s^{-1} in July. The SMC is sometimes separated from the coast of Sri Lanka by a coastal westward countercurrent bringing Bay of Bengal water. The annual mean flow past Sri Lanka was 2–3 Sv westward in 1993–1994. Numerical models show that these monsoon currents are driven by the large-scale tropical wind field. Contrary to the equatorial circulation where the semiannual period prevails, the annual component dominates the upper layer flow north of 4°N .

Currents South of the Equator

Apart from shipdrifts and satellite-tracked drifting buoys, there are no direct long-term current

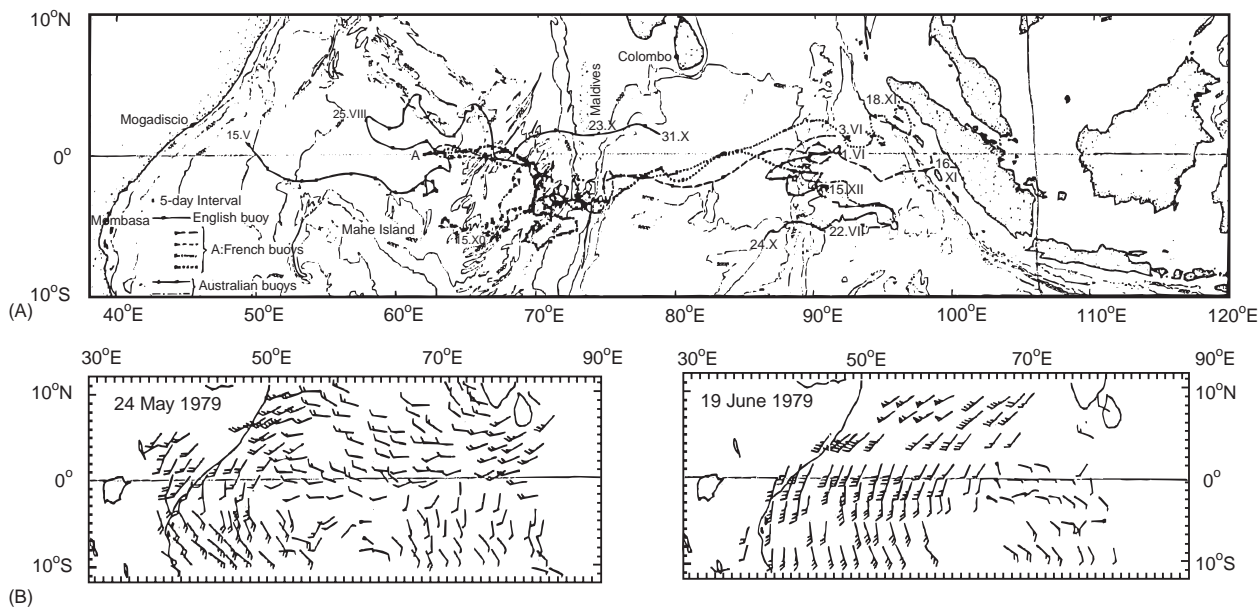


Figure 8 (A) Satellite-tracked drifting drogued (at 20 m) buoys trajectories in 1979; dots on the trajectories are spaced at 15-day intervals. (B) Wind vectors estimated from cloud trajectories on satellite images during the equatorial eastward wind period (24 May 1979) and during the fully developed SW monsoon (19 June 1979). (The short tick on the arrow corresponds to 5 knots, the longer one to 10 knots, and the triangle to 50 knots.) (Reprinted with permission from JR Luyten, M Fieux and J Gonella, *Equatorial currents in the Western Indian Ocean*, *Science* 209: 600–603, copyright 1980 American Association for the Advancement of Science.)

measurements in the South Equatorial Countercurrent and only two in the South Equatorial Current.

The South Equatorial Countercurrent

In contrast to the Pacific and the Atlantic oceans, where a countercurrent is found year-long north of the Equator between the North Equatorial Current and the South Equatorial Current, in the Indian Ocean the countercurrent is found south of the Equator and has a large extent only during a short period of the year.

During the winter monsoon, the Somali current flows southward, crosses the Equator, and merges with the northward flowing East Africa Coastal Current (EACC), at about 2–4°S, to form the eastward South Equatorial Countercurrent (SECC). It is a region of high eddy activity. The SECC is found between 2°S and 8°S during January–March. During that season the winds have an eastward component at those latitudes just north of the ITCZ. The speeds vary between 0.5 and 0.8 m s⁻¹ in the west, getting weaker in the east. In March 1995, at 80°E, observed surface velocities exceed 0.7 m s⁻¹ and the current extended to about 1100 m, with an eastward geostrophically deduced transport of about 55 Sv. In the east, part of it continues into the Java Current and part of it recirculates southward into the South Equatorial Current (SEC). It is detected in the

meridional slope of the thermocline which slopes downward toward the Equator, with an opposite upward slope of the sea surface (Figure 13). Together with the SEC and the EACC, the SECC forms an elongated cyclonic gyre.

In the latitude range about 10–13°S and between 20°S and 25°S, recent measurements of the sea level variability through satellite altimetry show westward propagation of sea level anomalies corresponding to semiannual and annual Rossby wave characteristics. The wind-driven model results show westward propagation of Rossby waves in the shear zone between the SECC and the SEC that are obstructed and partially reflected by the Mascarenes banks (55–60°E). In the west, at the end of the winter season, in March–April, when the eastward winds start on the equator, the outflow from the EACC into the SECC begins to move northward toward the Equator and the eastward flow at that time is mostly equatorial.

The South Equatorial Current

The westward South Equatorial Current forced by the south-east trade winds extends south of the SECC. It represents the northern branch of the South Indian subtropical gyre. It is seen in the meridional downward slope of the thermocline towards the south (Figure 13). It is partly fed, in

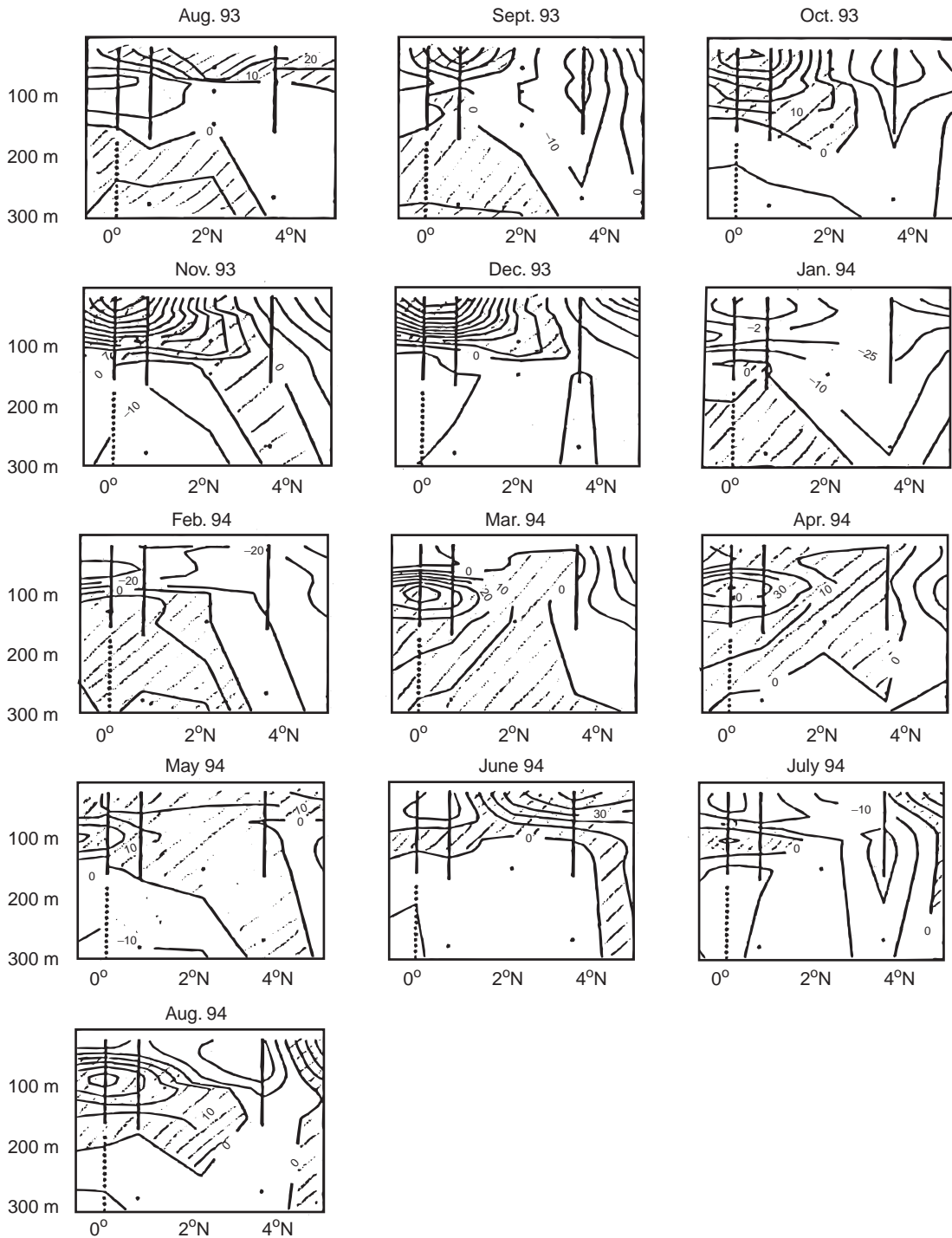


Figure 9 Monthly mean zonal velocities in cm s^{-1} for the upper 300m, south of Sri Lanka, along $80^{\circ}30'E$, between August 1993 and August 1994. Contour interval is 10 cm s^{-1} and shaded areas indicate eastward currents. Note the unusual reappearance of the EUC in August 1994. (From J Reppin, F Schott and J Fischer (1999) Equatorial currents and transports in the upper central Indian Ocean: Annual cycle and interannual variability, *Journal of Geophysical Research* 104(C7): 15495–15514, copyright by the American Geophysical Union.)

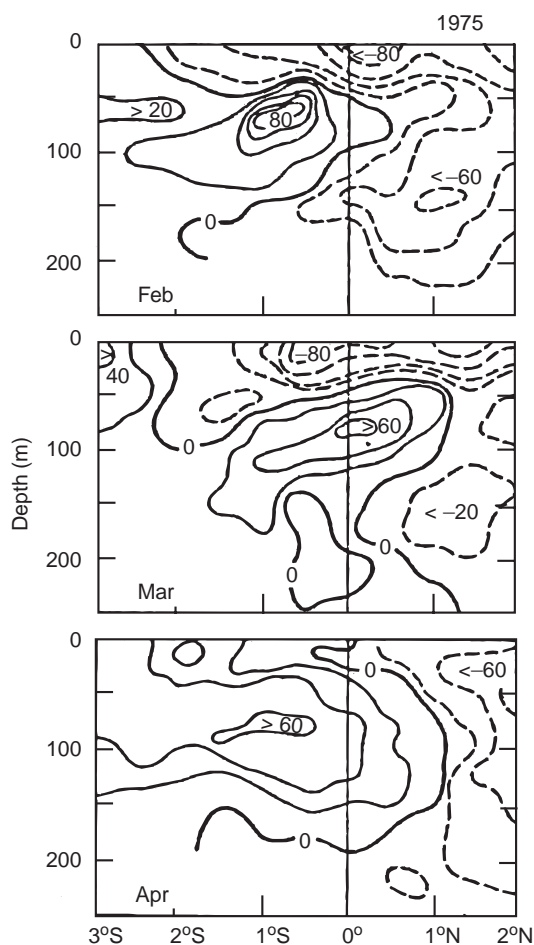


Figure 10 Meridional section along 53°E of zonal velocities in February, March, and April 1975 showing the equatorial undercurrent. Contours interval is 20 cm s^{-1} . Plain contours correspond to eastward currents and dashed contours to westward currents. (From A Leetmaa and H Stommel (1980) Equatorial current observations in the Western Indian Ocean in 1975 and 1976, *Journal of Physical Oceanography*, 10: 258–269, copyright by the American Meteorological Society.)

its northern part, between 10°S and 14°S , by the low-salinity throughflow jet originating from the western Pacific Ocean through the Indonesian Seas carrying about 4 to 12 Sv with larger extremes depending on the year. The low salinity extends down to about 1200 m. In March 1995, at 80°E , measured surface velocities reached 0.7 m s^{-1} . The SEC is the limit of the influence of the monsoon system and separates the northern and southern Indian Ocean. It is stronger during July–August when the SE trade winds are stronger. Its indirectly computed mean transport relative to the 1000 m level varies from 39 Sv in July–August to 33 Sv in January–February with large uncertainty. Its mean transport increases from east to west. Its latitudinal range varies between $8\text{--}22^{\circ}\text{S}$ in July–August and $10\text{--}20^{\circ}\text{S}$ in

January–February. Its velocities range between 0.3 m s^{-1} and 0.7 m s^{-1} .

The SEC impinges both on the east coast of Madagascar and on the east African coast, resulting in several intensified boundary currents along these coasts. East of Madagascar, the SEC splits near 17°S into a northward flow, carrying about 27 Sv near 12°S , and a southward flow, transporting 20 Sv between the surface and 1100 m near 23°S . At 12°S energetic boundary current transport variations occur at the 40–55-day period, contributing to about 40% to the total transport variance, while at 23°S the 40–55-day period fluctuations contribute only 15% to the total transport variance. The northern branch of the SEC splits again east of the African coast near Cape Delgado (11°S) into the southward flowing Mozambique Current (MC) and the northward flowing East African Coastal Current (EACC).

Drifting-buoy trajectories describe an elongated cyclonic gyre of the equatorial current system composed of the equatorial eastward jet or the SECC, depending on the season, the off Sumatra SE current, the westward SEC, and the EACC. Some drifting buoys, launched during a transition period at the Equator, carried into the eastward Wyrki jet and in the SECC, crossed the basin, then were driven south-eastward into the Sumatra current, then crossed the basin westward into the SEC, and flowed back to the Equator in the western region exactly one year later when they were again carried into the SECC (Figure 14).

Conclusion

Owing to stronger winds in the tropical Indian ocean, the currents are stronger than in the Pacific and Atlantic Oceans but seasonally are highly variable. Away from the western boundary the equatorially trapped long waves (Kelvin and Rossby) explain most of the observed seasonal variations of the equatorial currents.

In contrast to the Atlantic and Pacific Oceans, equatorial upwelling is weak in the Indian Ocean. During the period of strong current, the surface flow is eastward, associated with a strong convergence at the surface inducing an equatorial downwelling. The upwelling regions are found instead north of the equator, along the Somalia, the Arabian, and the Indian coasts, and are seasonally depending.

The equatorial current structure in the Indian ocean is complex and further long-term observations as well as modeling efforts are needed to better understand its seasonal and interannual variability and its role in the large-scale meridional exchanges between the northern and the southern Indian Ocean.

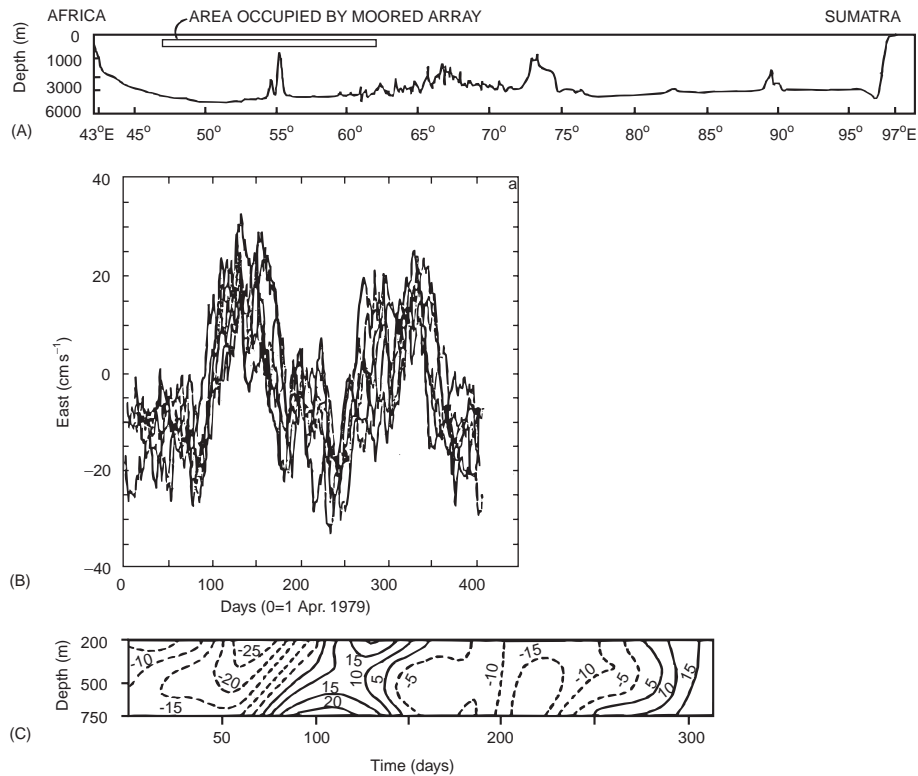


Figure 11 (A) Vertical section of the Indian Ocean along the Equator with the location of the current-meter array between 47°E and 62°E. (B) Time series of east velocity from seven current-meters at 750m depth starting on April 1 1979. (C) Contour plot of low-frequency east velocity as a function of depth and time (day 0 = 1 April 1979). At each nominal depth (200, 500, 750 m), four records are filtered by a 30-day running mean and averaged together. The contour interval is 5 cm s⁻¹. (From JR Luyten and DH Roemmich (1982) Equatorial currents at semiannual period in the Indian Ocean, *Journal of Physical Oceanography* 12: 406–413, copyright by the American Meteorological Society.)

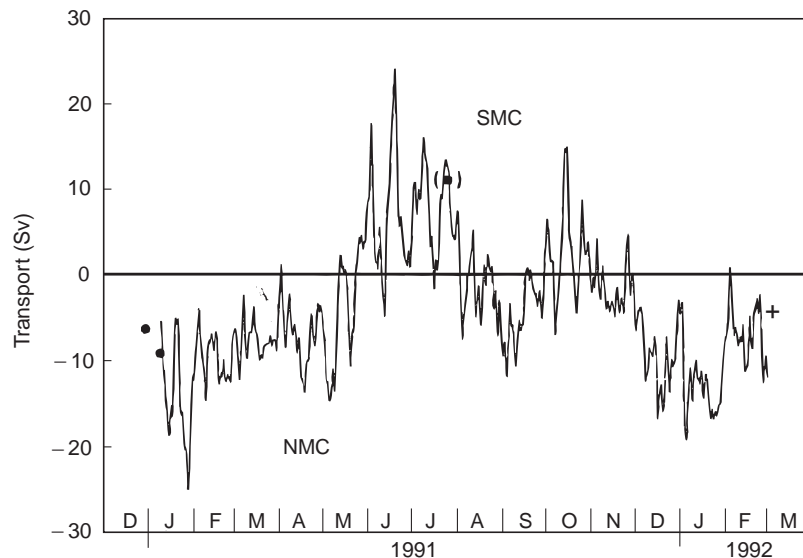


Figure 12 Seasonal variability of the transport in the upper 300m from moorings south of Sri Lanka, between 3°45'N and 5°52'N, in 1991–1992. (The solid circles are from ship-mounted acoustic Doppler current profiler measurements in December 1990–January 1991; the solid circle in parentheses is for July 1991, and the cross is from Pegasus profiler measurements in March 1992.) (From F Schott, J Reppin, J Fisher and D Quadfasel (1994) Currents and transports of the monsoon current south of Sri Lanka, *Journal of Geophysical Research* 99(C12): 25127–25141, copyright by the American Geophysical Union.)

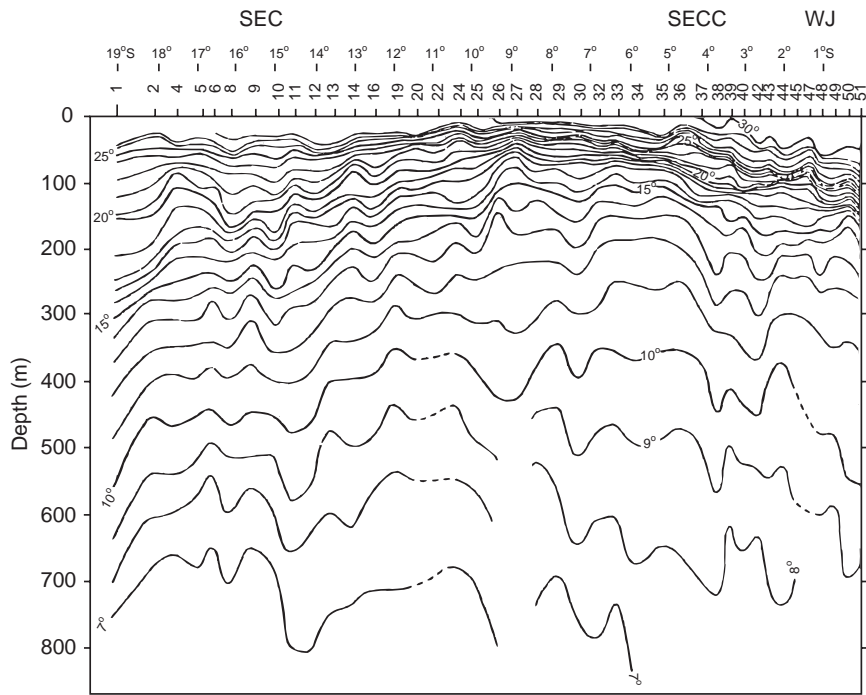


Figure 13 Meridional temperature section along 54–55°E in May 1981 with 1°C isotherm interval. The downward slope of the thermocline from 9°S toward the south corresponds to the SEC, and the downward slope toward the Equator corresponds to the SECC. Close to the Equator, the accentuated slope corresponds to the May Wyrki jet. (From M Fieux and C Levy (1983) Seasonal observations in the western Indian Ocean. In: *Nihoul JCJ (ed.) Hydrodynamics of the Equatorial Ocean*. Amsterdam: Elsevier Science, 17–29.)

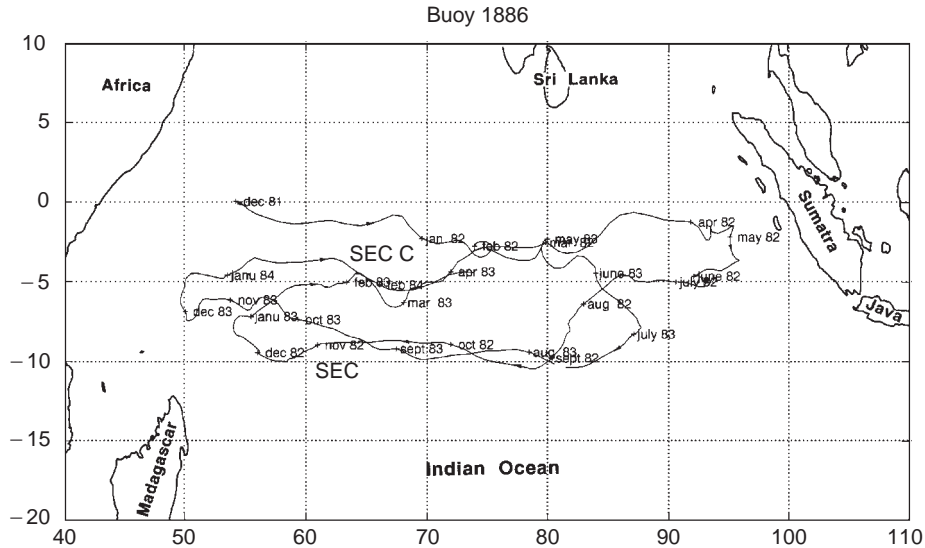


Figure 14 Satellite-tracked drifting buoy trajectory between November 1981 and February 1984. The buoy, drouged at 20m, was entrained eastward in the November jet then in the SECC and back westward into the SEC. One year later it was again entrained in the same elongated gyre. (From M Fieux (1987) *Océan Indien et Mousson*, ‘Unesco Anton Bruun Lecture’, unpublished manuscript.)

See also

Agulhas Current. Coastal Trapped Waves. Current Systems in the Indian Ocean. Elemental Distribution: Overview. El Niño Southern Oscillation (ENSO). Indonesian Throughflow and Leeuwin Current. Rossby Waves. Somali Current. Thermohaline Circulation. Water Types and Water Masses. Wind Driven Circulation.

Further Reading

Cutler AN and Swallow JC (1984) *Surface Currents of the Indian Ocean (to 25°S, 100°E): Compiled from Historical Data Archived by the Meteorological Office, Bracknell, UK*. Wormley, UK: Institute of Oceanographic Science (unpublished report) 187, 8pp. and 36 charts.
 Fein JS and Stephens PL (eds) (1987) *Monsoons*. Washington DC: NSF and Wiley.
 Open University, Oceanography Course Team (1993) *Ocean Circulation*. Oxford: Pergamon Press.
 Tomczak M and Godfrey S (1994) *Regional Oceanography: An Introduction*. Oxford: Pergamon Elsevier.